CrystEngComm

Accepted Manuscript

ROYAL SOCIETY OF CHEMISTRY

www.rsc.org/crystengcomm

Journal Name

COMMUNICATION

Hierarchical structures of self-assembled hybrid calcium carbonate: nucleation kinetic studies on biomineralization

Received 00th January 20xx,
Accepted 00th January 20xx

DOI: 10.1039/x0xx00000x

www.rsc.org/

Jiadong Fan, Yang Zhang, Nianjing Ji, Xiulan Duan, Hong Liu, Jiyang Wang and Huaidong Jiang*

A novel $CaCO_3$ hybrid material with well-ordered hierarchical structure was synthesized under the effects of phosvitin. Kinetic experiments demonstrate that phosvitin suppresses the supersaturation-driven interfacial structure mismatch between $CaCO_3$ crystallite and substrate, and promotes the formation of oriented $CaCO_3$ nanocrystallite assemblies at low supersaturations.

Many organisms are capable of fabricating high performance materials with synergetic structures under very moderate conditions via biomineralization.[1-8] These exquisite hierarchical structures formed during natural processes, as a guide for new materials technology, have attracted much attention for over a century, because they often exhibit far superior properties to artificial materials.[9-13] Understanding and mimicking the process of biomineralization are hence critical to biomimetic materials science for inorganic-organic hybrid materials, biocompatible materials, and biomedical engineering of hard tissues.[14-20] Inspired by biology, efforts are under way to unravel the strategy adopted by nature in terms of nano-composites, self-assemblies and hierarchical structures. Although previous studies have shown that certain biomacromolecules are involved in mediating mineralization via the effects of templates and facilitating the construction of organized self-assembled structures,[21-24] a few key questions are still not fully understood. For example, how are biomineral nanocrystallites kinetically assembled to form hierarchical structures? How do biomolecules mediate mineralization, in particular with regards to the detailed nucleation kinetic processes and the interfacial structural correlation between biomolecule and biomineral?

Here we, for the first time, report $CaCO_3$ nanocrystallite assemblies with well-ordered hierarchical structure synthesized under the effects of phosvitin, which is one of the most phosphorylated proteins in nature and widely found in egg yolk. We subsequently elucidate the mechanism of the self-organized $CaCO_3$ assemblies from viewpoints of kinetics, interfacial structure and properties.

[a] State Key Laboratory of Crystal Materials, Shandong University, Jinan 250100, China. E-mail: hdjiang@sdu.edu.cn

† Electronic Supplementary Information (ESI) available: [details of any supplementary information available should be included here]. See DOI:

Experimental

The biomineralization of self-organized $CaCO_3$ assemblies was studied under different conditions. We synthesized a series of $CaCO_3$ precipitates from various supersaturated solutions by using $CaCl_2$ and NH_4HCO_3, with and without phosvitin (75 mg·L^{-1}) at room temperature. The precipitate was quickly washed with deionized water and acetone, and subsequently dried. The microstructure of $CaCO_3$ assemblies obtained from the solutions was imaged using a scanning electron microscope (SEM, JSM-6700F, JEOL) after coating with platinum.

Equilibrium dialysis of phosvitin was performed with the dispo-equilibrium dialyzers consisting of two chambers separated by a dialysis membrane with a molecular mass cutoff of 5 kDa. The apparatus for equilibrium dialysis was washed with 10 mM EDTA, followed by an extensive wash with deionized water. The upper chamber was filled with phosvitin solution with a concentration of 100 mg·L^{-1}. The bottom chamber was filled with the dialysis buffer containing $CaCl_2$ varying from 10 μM to 3 mM plus trace $^{45}CaCl_2$ (Amersham Biosciences). Dialysis was carried out for 24 hours at room temperature, and the radioactivity from ^{45}Ca in the bottom and the upper chambers was measured by using a Beckman LS-6500 liquid scintillation counter. The bound and free Ca^{2+} was then counted, and the dissociation constant, K_d, was determined by Scatchard analysis.[25]

The nucleation kinetics experiments of $CaCO_3$ were performed on a dynamic light-scattering system (DLS, BI-200SM, Brookhaven Instruments), which allows an in situ measurement of the nucleation process. In order to study the effects of phosvitin on the nucleation kinetics of $CaCO_3$, the nucleation induction time t_s at various supersaturations was measured in control solutions without additives and in the presence of phosvitin (2.5mg·L^{-1}) by using DLS.

Results and Discussion

Figure 1a shows SEM images of $CaCO_3$ crystals grown from the solution without any additives, whereas for comparison purposes a single calcite crystal is shown in Fig. 1a inset. A typical rhombohedra morphology consisting of six basal (104) planes of $CaCO_3$ single crystal is consistent with the trigonal crystallographic characteristics

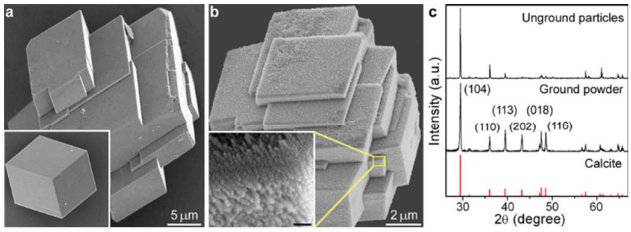

Fig. 1 (a) SEM images of $CaCO_3$ crystals grown in solutions without additives. Inset shows a single calcite crystal. (b) SEM images of self-assembled hybrid $CaCO_3$ with long-range-ordered hierarchical structures formed in solution with phosvitin. A zoomed image (inset) indicates that the faceted "crystal" is composed of well-ordered nanocrystallites. Scale bar is 100 nm. (c) XRD patterns of unground and ground crystal-like hybrid materials and a standard pattern for calcite.

of calcite, which was further confirmed by X-ray diffraction (XRD) analysis. In the presence of phosvitin, the microstructure of $CaCO_3$ formed in the solution (Fig. 1b) is distinctively different from that of common, smooth crystals grown from the pure solution. One of the most surprising features is the formation of crystal-like hybrid $CaCO_3$ materials with hierarchical structures. Figure 1b inset shows that the self-assembled material is composed of well-ordered nanocrystallites. In this respect, they are also different from previously reported calcite crystals.[26,27] The XRD pattern of the finely ground sample (Fig. 1c middle) shows strong diffraction peaks, which matches the standard XRD pattern of calcite (Fig. 1c bottom), indicating that the hybrid material belongs to calcite. In contrast, the XRD pattern of unground hybrid $CaCO_3$ particles only shows a few strong diffraction peaks (Fig. 1c top), which implies that the organization of the nanocrystallites within the self-assembled material (Fig. 1b inset) are not random but well-oriented.

To investigate the novel hierarchical structures, we analyzed the microstructure of the hybrid materials formed under different conditions. Figure 2a shows the surface and internal structures of a typical hybrid material synthesized in a relatively low-supersaturated solution. Zoomed-in SEM image (Fig. 2b) shows that the faceted and porous assemblies are composed of well-organized nanocrystallite clusters although the ultrastructure of nanocrystallites doesn't indicate typical morphology of crystal on the nanometer scale (Fig. 2b inset)**.** The inner structure shows that the nanoclusters are long-range-ordered along certain directions within the hybrid materials (labeled with an arrow). Figures 2c and d show the microstructure of a $CaCO_3$ particle formed in a solution with relatively high supersaturation. The particle has rough surfaces but more regular calcite morphology and straight crystal edges. In comparison with particle shown in Fig. 2b, the microstructure becomes more compact between the nanocrystallite clusters.

The chemical composition of the hybrid materials was measured using energy dispersive x-ray spectroscopy (Supplementary Information), indicating that the concentration of calcium in hybrid nanocrystallites is about twice higher than that in controlled samples. Since phosvitin is heavily phosphorylated and has a negative charge density, we investigated the calcium binding capacity of the phosvitin. Equilibrium dialysis was carried out using a microdialyzer system and the results are shown in Fig. 3a. The data obtained from the dialysis enable one to determine the dissociation constant (K_d) and the number of binding sites.[25] As shown in a Scatchard plot (Fig. 3a inset), phosvitin exhibits a markedly biphasic Ca^{2+} binding within the Ca^{2+} concentration measured. This implies that phosvitin contains two Ca^{2+} binding sites with different affinities in the measuring range. These data fit well with the two-site binding model and yielded a high-affinity Ca^{2+}

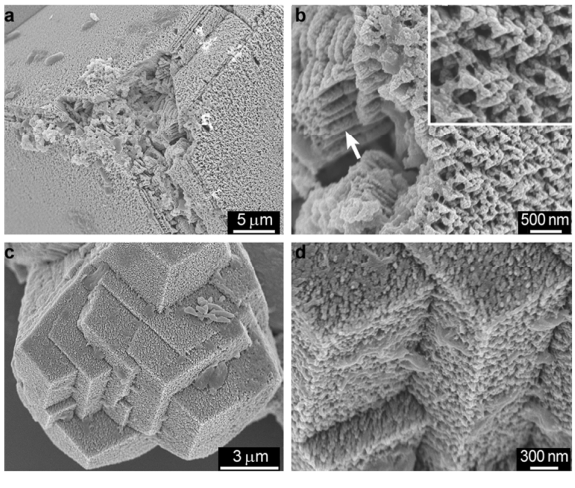

Fig. 2 SEM images of self-assembled $CaCO_3$ hybrid materials synthesized from (a) low and (c) relatively highly supersaturated solutions in the presence of phosvitin. (b) and (d), zoomed-in SEM images of (a) and (c), show that faceted and porous crystal-like surface is composed of well-ordered nanocrystallite clusters.

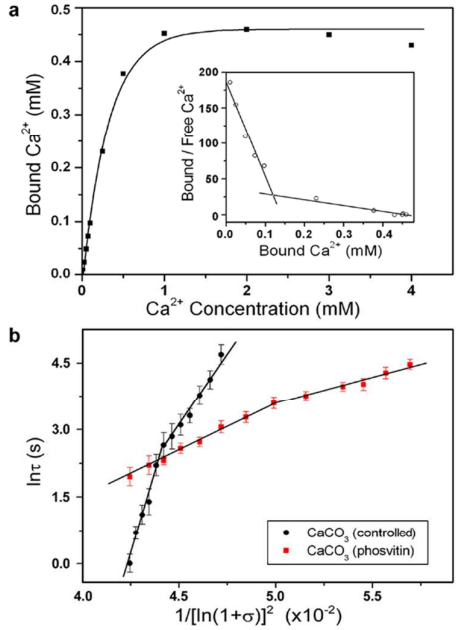

Fig. 3 Effects of phosvitin on binding of Ca^{2+} and nucleation kinetics. (a) Ca^{2+} binding curve of phosvitin, determined by equilibrium dialysis with $^{45}Ca^{2+}$. Each point represents an average value of three independent measurements. Inset, Scatchard plot for Ca^{2+} binding capacity of phosvitin. (b) DLS measurements of $CaCO_3$ nucleation under different conditions.

binding site (K_d = 0.73 μM) and a modest-affinity Ca^{2+} binding site (K_d = 10.1 μM). The results from the dialysis experiments are consistent with EDX and zeta potential measurements (Supplementary Information), which indicates that phosvitin has a strong interaction with calcium ions. The presence of the molecules hence facilitates the nucleation of $CaCO_3$ in solutions by binding with Ca^{2+} and produces locally a high degree of supersaturation.[28,29]

To study the formation of the well-ordered self-assemblies, we examined nucleation kinetics using a dynamic light-scattering (DLS) system.[28-30] The induction time (t_s) of the nucleation was measured at different supersaturations (σ) to determine the kinetics of biomineralization. For the heterogeneous nucleation, the slope of the $\ln(t_s)$ vs $1/[\ln(1+\sigma)]^2$ plot[28-30] (Fig. 3b) was obtained from the interfacial correlation factor $f(m)$[30] which was used to characterize the interaction and structural match between nucleating phase and substrate. For a given system, $f(m) \rightarrow 0$ represents the strongest average interaction and the optimal structure match between the nucleating phase and the substrate, whereas $f(m) \rightarrow 1$ represents a deteriorating structural match amounting to structural mismatch.[29] As shown in Fig. 3b, the controlled curve, corresponding to the solution without any additives, can in principle be fit by two intersecting straight lines with different slopes. With the increase of supersaturation, $f(m)$ increases from $6.78\times10^2\ \kappa^{-1}$ to $1.47\times10^3\ \kappa^{-1}$ accordingly, where κ is a constant for a given system. This implies that the interfacial structural correlation between the nucleating phase and the substrate (*i.e.* existing crystallites, bubbles, etc.) changes with the increase of supersaturation from a state of structural match to a state of structural mismatch.[30] This so-called supersaturation-driven interfacial structural mismatch[28] demolishes the formation of the highly ordered $CaCO_3$ crystallite assemblies at high supersaturations. However, in the presence of phosvitin (C = 2.5 mg·L^{-1}), the $\ln t_s$ vs $1/[\ln(1+\sigma)]^2$ plot gives rise to two straight lines with smaller slopes shown in Fig. 3b, indicating better interfacial structure match. In comparison with the controlled curve, the presence of phosvitin also stretches the structural match domain toward higher supersaturations. This indicates that phosvitin suppresses or buffers the supersaturation-driven structural mismatch, allowing the self-epitaxial mediated and well-ordered $CaCO_3$ crystallite assemblies to form in a much wider range of supersaturations.

In order to further understand the formation mechanism of the well-organized hierarchical $CaCO_3$ assemblies (Figs. 1b and 2), we propose a model based on kinetic behavior of nucleation and growth. As shown in Fig 2S (Supplementary Information), with the increase of supersaturation, different self-assembled $CaCO_3$ is formed through supersaturation-driven crystallographic mismatch nucleation and growth in solutions without any additives.[29] The kinetics of this type of heterogeneous nucleation depends on the surface supersaturation of the growing/existing crystal, which increases monotonically with bulk supersaturation. When the supersaturation is very low (regime *I* in Fig. 2S, ESI†), $CaCO_3$ single crystals with typical rhombohedra morphology normally grow due to a high energy barrier of nucleation (ΔG^*). Crystallographic mismatch nucleation can only take place on an existing crystal surface when the surface supersaturation is larger than a critical value (σ_c). In that case, the barrier of mismatch nucleation (ΔG^*_{mis}), will drop rapidly with the increase of supersaturation,[29,30] and the interface structural match between the existing crystals and the nucleating phases will deviate from the optimal crystallographic structural match position (regime *II* in Fig. 2S, ESI†).[29] Therefore, the architecture of assemblies varies from ordered crystallites with the same orientation on the surfaces of existing crystals to loose and random amorphous aggregations, due to high nucleation rate and poor structural match.

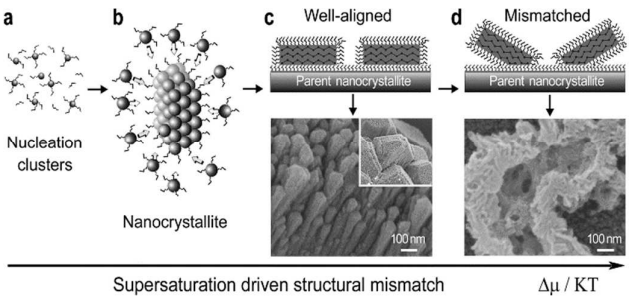

Fig. 4 Illustration of heterogeneous nucleation and growth of self-assembled $CaCO_3$ from aqueous solutions with phosvitin.

Figure 4 shows a schematic of the nucleation and growth mechanism of $CaCO_3$ from aqueous solutions with phosvitin. At an early stage of crystallization, strong interaction between phosvitin and calcium facilitates the nucleation of $CaCO_3$ in solution by producing locally a high degree of supersaturation (Fig. 4a). Once $CaCO_3$ nuclei occur in the solution, phosvitin adsorbed on the surfaces of the nuclei not only influences the interfacial structure and properties, but also exerts a negative impact on the surface integration. That is to say, the growth rate is significantly reduced due to adsorption of additives on the surface of a growing nucleus, which temporally stabilizes nanocrystallites of $CaCO_3$ (Fig. 4b).[15,31]

With further crystallization, the primary nanocrystallites get covered by phosvitin due to the negatively charged surfaces. Kinetically, the occurrence of phosvitin lowers the nucleation barrier, resulting in an increase of nucleation rate. Apart from this, slow surface integration kinetics gives rise to a high surface supersaturation. Thus a small-angle structure mismatch nucleation is easily triggered on the surface of a growing crystallite at low supersaturations. The typical crystallite patterns are illustrated in Fig. 4c. As the nucleation and growth of nuclei proceed further, a well-orientated nanocrystallite assembly is formed by the growth and coalescence of crystallites on the surface of the modified substrate (Fig. 4c bottom). At relatively high supersaturations, the requirement of the structural match between the daughter and the parent crystals becomes less strict due to a sharp drop in ΔG^*_{mis}. Therefore, the so-called wide-angle structural mismatch branching occurs, shown in Fig. 4d. This can even result in aggregations of amorphous $CaCO_3$ clusters due to high nucleation rate and poor structure match at very high supersaturations. In this case, crystallite patterns become open, random and highly branched crystallite networks (Fig. 4d bottom). Based on the above analysis, we conclude that kinetic nucleation and growth, especially mismatch nucleation play an important role in the formation of these self-organized nanocrystallite assemblies by controlling the supersaturation and interfacial structural correlation.

Conclusions

As a widespread strategy in organisms, biomineralization reveals an astonishing diversity of biominerals and microarchitectures containing specially adapted physical properties. We reported a novel $CaCO_3$ hybrid materials with well-ordered hierarchical structures synthesized by using the protein of phosvitin. The self-assembly of the hierarchical structures was elucidated by a unique synergistic mechanism: kinetically driven nucleation and phosvitin-mediated mineralization. We demonstrated that proteins, such as phosvitin, can suppress the supersaturation-driven interfacial structure mismatch between the crystallite and the substrate, and facilitate the formation of well-ordered nanocrystallite assemblies with hierarchical structures at low supersaturations. These results will not only improve our understanding of hierarchical architectures in biomineralization, but also provide guidance for designing and engineering highly ordered organic-inorganic hybrid materials.

Acknowledgements

We thank Prof. X. Y. Liu for many stimulating discussions. This work was supported by the National Natural Science Foundation of China (31430031, U1332118), the National Science Foundation of Shandong Province (JQ201117), and the Program for New Century Excellent Talents (NCET-11-0304).

Notes and references

1 H. A. Lowenstam and S. Weiner, On biomineralization, Oxford University Press, New York 1989.
2 X. Fei, W. Li, Z. Shao, S. Seeger, D. Zhao and X. Chen, *J. Am. Chem. Soc.*, 2014, **136,** 15781-15786.
3 Y. Oaki, M. Kijima and H. Imai, *J. Am. Chem. Soc.*, 2011, **133**, 8594-8599.
4 C. S. Chan, G. De Stasio, S. A. Welch, M. Girasole, B. H. Frazer, M. V. Nesterova, S. Fakra and J. F. Banfield, *Science*, 2004, **303**, 1656-1658.
5 J. Aizenberg, A. Tkachenko, S. Weiner, L. Addadi and G. Hendler, *Nature*, 2001, **412**, 819-822.
6 H. C. Lichtenegger, T. Schoberl, M. H. Bartl, J. H. Waite and G. D. Stucky, *Science* 2002, **298**, 389-392..
7 S. Kamat, X. Su, R. Ballarini, A. H. Heuer, *Nature*, 2000, **405**, 1036-1040.
8 H. D. Jiang, D. Johnson, C. Song, B. Amirbekian, Y. Kohmura, Y. Nishino, Y. Takahashi, T. Ishikawa and J. Miao, *Phys. Rev. Lett.*, 2008, **100**, 038103.
9 L. Addadi, J. Aizenberg, E. Benash and S. Weiner, Crystal engineering: from molecules and crystals to materials, (Eds**:** D**.** Braga**,** F**.** Grepioni and A. G. Orpen), Kluwer Academic Publishers, Dordrecht 1999.
10 E. Bäuerlein, *Angew. Chem. Int. Ed.*, 2003, **42**, 614-641.
11 M. L. Snead, *Connect Tissue Res.*, 2003, **44**, 47-51.
12 F. H. Wilt, C. E. Killian and B. T. Livingston, *Differentiation*, 2003, **71**, 237-250.
13 A. P. Jackson, J. F. V. Vincent and R. M. Turner, *Proc. R. Soc. Lond. B*, 1988, **234**, 415-440.
14 S. Gajjeraman, K. Narayanan, J. Hao, C. Qin and A. George *J. Biol. Chem.*, 2007, **282**, 1193-1204.
15 K. Subburaman, N. Pernodet, S. Y. Kwak, E. DiMasi, S, Ge, V. Zaitsev, X. Ba, N. L. Yang and M. Rafailovich, *Proc. Natl. Acad. Sci. USA*, 2006, **103**, 14672-14677.
16 H. Colfen and S. Mann, *Angew. Chem. Int. Ed.*, 2003, **42**, 2350-2365.
17 K. Naka and Y. Chujo, *Chem. Mater.*, 2001, **13**, 3245-3259.
18 J. Zhan, H. P. Lin and C. Y. Mou, *Adv. Mater.*, 2003, **15**, 621-623.
19 A. M. Belcher, A. M. Belcher, X. H. Wu, R. J. Christensen, P. K. Hansma and D. E. Morse, *Nature*, 1996, **381**, 56-58.
20 R. F. Service *Science*, 1999, **286**, 2442-2444.
21 G. Greenfield, D. C. Wilson and M. A. Crenshaw, *Am. Zool.*, 1984, **24,** 925-932.
22 S. Mann, *Nature*, 1988, **332,** 119-124.
23 L. Addadi and S. Weiner, *Proc. Natl. Acad. Sci. USA*, 1985, **82,** 4110-4114.
24 E. Pouget, E. Dujardin, A. Cavalier, A. Moreac, C. Valéry, V. Marchi-Artzner, T. Weiss, A. Renault, M. Paternostre and F. Artzner, *Nature Mater.*, 2007, **6**, 434-439.
25 G. Scatchard, *Ann. NY. Acad. Sci.*, 1949, **51**, 660-672.
26 S. Burazerovic, J. Gradinaru, J. Pierron and T. R. Ward, *Angew. Chem. Int. Ed.*, 2007, **46**, 5510-5514.
27 J. J. J. M. Donners, R. J. M. Nolte and N. A. J. M. Sommerdijk, *J. Am. Chem. Soc.*, 2002, **124**, 9700-9701.
28 X. Y. Liu and C. S. Strom, *J. Chem. Phys.*, 2000, **112**, 4408-4411.
29 H. D. Jiang and X. Y. Liu, *J. Biol. Chem.*, 2004, **279**, 41286-41293.
30 X. Y. Liu, *Advances in Crystal Growth Research*, (Eds: K. Sato, K. Nakajima and Y. Furukawa), Elsevier Science, Amsterdam 2001.
31 A.W. Xu, Y. Ma and H. Colfen, *J. Mater. Chem.* 2007, **17**, 415-449.G. Scatchard, *Ann. NY. Acad. Sci.*, 1949, **51**, 660-672.

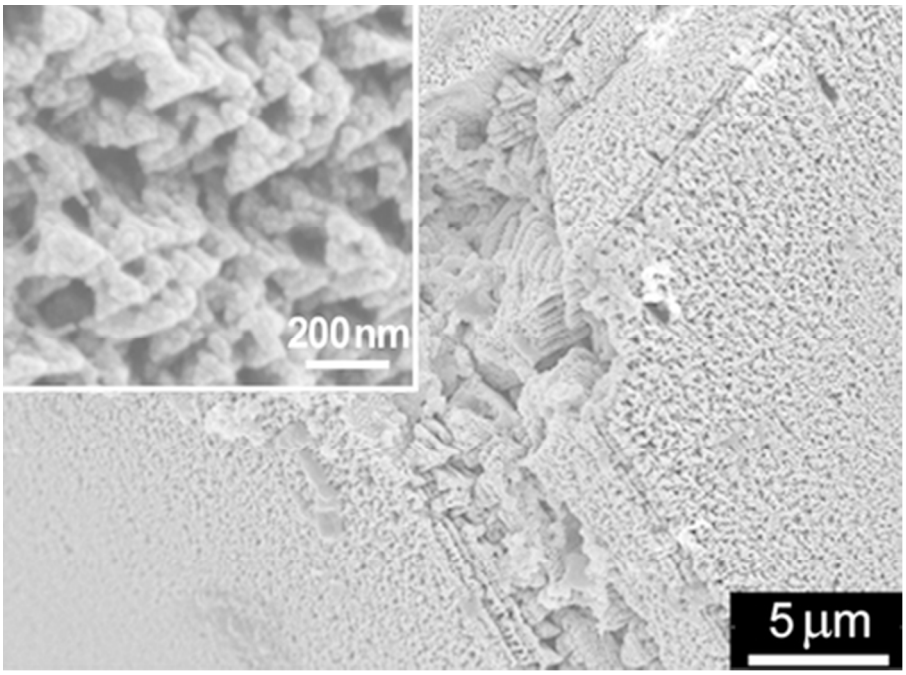

The mechanism of self-assembled $CaCO_3$ hierarchical structures was elucidated from the viewpoints of kinetically driven nucleation and phosvitin-mediated mineralization.
38x28mm (300 x 300 DPI)